Theoretical Chemistry Accounts (2023) 142:13
https://doi.org/10.1007/s00214-022-02949-8

RESEARCH

Dominant changes in centre Fe atom of decamethyl-ferrocene from ferrocene in methylation

Feng Wang[1] · **Christopher T. Chantler**[2]

Received: 1 October 2022 / Accepted: 23 December 2022

Abstract

Staggered decamethyl-ferrocene (*Fc) becomes the lower energy conformer at low temperature, whereas the eclipsed conformer of ferrocene (Fc) is more stable. The powerful infrared (IR) spectroscopy which has remarkably provided signatures of ferrocene (Fc) in eclipsed and staggered conformers recently is employed to investigate methylation of Fc. The most significant consequences of the full methylation of Fc in the IR spectra are the blue shift of the band at ~ 800 cm^{-1} in Fc to ~ 1500 cm^{-1} in *Fc, and the enhancement of the C–H stretch band at ~ 3200 cm^{-1} region in *Fc. Further analysis reveals large impact of Fc methylation on core electron energies of the centre Fe atom ($1s^2 2s^2 2p^6 3s^2 3p^6$). The Fe core electron energy changes can be as large as ~ 10 kcal mol^{-1} and are directional—the Fe $2p_z$ and $3p_z$ orbitals along the *Cp–Fe–*Cp axis (Cp centroids, vertical) change more strongly than other Fe core electrons in p_x and p_y orbitals. The directional inner shell energy changes are evidenced by larger inner shell reorganization energy. Energy decomposition analysis (EDA) indicates that methyl groups in *Fc apparently change the physical energy components with respect to Fc. The large steric energy of *Fc evidences that the closest hydrogens on adjacent methyl groups of the same *Cp ring in crystal structure are 0.2–0.4 Å closer than the hydrogens on nearest-neighbour methyl groups on opposing rings in *Fc. A significant increase in Pauli repulsive energy contributes to the large repulsive steric energy in *Fc.

Keywords Decamethylferrocene (*Fc) · Ferrocene (Fc) · Fe · DFT calculations · IR spectrum · Excess orbital energy · Energy decomposition analysis (EDA)

1 Introduction

Contemporary organometallic chemistry was inaugurated by the discovery of ferrocene $Fe(C_5H_5)_2$, i.e., dicyclopentadienyl iron ($FeCp_2$ or Fc). Since its discovery [1, 2], Fc opened up new areas of chemistry, deepened our understanding of structure, bonding, and reactivity, and hence paved the way for the burgeoning field of organometallic chemistry itself [3]. Fc has stimulated an immense number of studies on cyclopentadienyl (Cp) and other symmetrically delocalized hydrocarbon metal complexes with a unique sandwich molecular structure, strong metal-ring π bonding, facile redox behaviour, and ease of derivatization [4]. It has wide applications including catalytic stereoselective and asymmetric transformations, materials science, crystal engineering, bio-organometallic chemistry, electrochemistry especially in electron transfer processes, biochemistry, organic synthesis, polymer chemistry, fuel additives and drug design and development [3, 5]. As a result, Fc studies have contributed to the rapid growth and hence rapidly moving frontiers of this family of compounds during the past several decades [3].

Ferrocene and ferrocene-based molecules are not mere trophy molecules for the shelf [3]; they are also amongst the most difficult organometallic complexes in chemistry and materials science. From the beginning, the symmetry of ferrocene was a central issue in its structural exploration. Two main conformers were predicted: the eclipsed (D_{5h}) and

This article is in honour of Professor Pratim Kumar Chattaraj on the occasion of his 65th birthday, for his contributions to Theoretical and Computational Chemistry.

✉ Feng Wang
fwang@swin.edu.au

[1] Department of Chemistry and Biotechnology, School of Science, Computing and Engineering Technologies, Swinburne University of Technology, Hawthorn, Melbourne, VIC 3122, Australia

[2] School of Physics, The University of Melbourne, Parkville, VIC 3010, Australia

Published online: 13 January 2023

staggered (D_{5d}) Fc produced by the positions of the parallel cyclopentadienyl rings, which has caused a significant challenge for the study of Fc since its discovery [1, 2]. The debate on the most stable conformer of Fc, whether it is the eclipsed (D_{5h}) or the staggered (D_{5d}), has been raised by a number of studies using combined DFT calculations and experimental measurements [6–10]. A new careful analysis of IR spectra has provided the strongest evidence so far of the stability of the eclipsed conformation at lower temperatures for Fc [6, 12]. The studies reveal that the conformational interchange process from eclipsed Fc to staggered Fc involves a twist around the C_5 rotation axis that changes the torsion angle connecting any carbon atom of one ring to the corresponding carbon atom of the second ring through the two ring centroids [11]. Kaspi-Kaneti and Tuvi-Arad further indicated that the symmetry transition point cusp at 18° represents the point at which the molecular geometry has an equal distance from an eclipsed and staggered Fc [11]. These conclusions are confirmed by our most recent first principle molecular dynamics study [12] which also revealed that conformational changes of ferrocene with temperature and confirmed by the most recent study when Fc crystallised with hexafluorobenzene of Bear et al. [13].

The density functional theory (DFT) study [6] discovered that the infrared (IR) spectra of Fc contain the clearest signatures of the Fc conformers. The earlier IR measurements of Fc of Lippincott and Nelson [14] achieved an amazing accuracy, decades before the synchrotron-based Fourier transform FTIR technology became available. However, despite the accuracy in the IR measurements of Fc, the IR spectra of Fc were assigned to the staggered (D_{5d}) Fc conformer [14] due in part to the lack of sufficiently accurate theoretical support. The IR signature of Fc has now been accurately determined and confirmed [7, 10].

Detailed structural understanding of the Fc complex is very important as its derivatives may inherit particular properties which only exist in a particular conformer [15]. For example, additional ligands coordinating to the metal and the Cp rings while maintaining certain symmetry can be a geometric requirement for the D_{5h} conformer [15]. Design of synthesis pathways and understanding of the mechanics and reaction dynamics of the Fc derivatives require detailed information of the structure, symmetry and property of the Fc conformers. The stability of eclipsed and staggered conformers of Fc has been a challenge issue and was defined as either eclipsed or staggered in many textbooks [16]. Recent articles of Coriani et al. [17] Roy et al. [18], Gryaznova et al. [19] and Bean et al. [20] have well documented the history and earlier status of the Fc studies.

Ferrocene and derivatives have attracted extensive attention to their peculiar chemical structure and biological activities [5]. Full methylation of Fc by replacing all hydrogen atoms with methyls ($-CH_3$) produces decamethyl-ferrocene ($Fe(C_5(CH_3)_5)_2$, *Fc), although the latter (*Fc) is produced on treating iron(II) chloride with $Li[C_5(CH_3)_{55}]$ [21]. There exists a large number of studies of the structure and spectroscopy of Fc and *Fc [8, 9, 19, 22–25], which reported that *Fc is more stable in staggered conformer in gas phase [9, 10], in the frozen solutions [8] and in the crystal [24]. When applying high-accuracy X-ray absorption fine structure (XAFS) of Fc and *Fc, clear evidence for the eclipsed conformation for Fc and the staggered conformation for *Fc for frozen solutions at ca. 15 K [8]. The rotational barrier of *Fc conformers was further determined to be 4.2 (1.3) kJ mol^{-1} in the crystal form by Freyberg et al. [24]. However, in terms of the structural parameters, Fc and *Fc are statistically very similar. In the present study, accurate DFT methods which have been validated with high-resolution FTIR experimental measurements [6, 7, 10] and XAS experimental measurements [8, 9] are employed in the calculations.

2 Computational methods

In order to reveal the differences between *Fc and Fc with minimum environmental impact, both Fc and *Fc compounds are studied in isolation. The eclipsed and staggered conformer geometries of *Fc were optimized using the B3LYP/m6-31G(d) model, which is the same as the model previous employed to study Fc conformers in gas phase [6]. This m6-31G(d) basis set incorporates necessary diffuse d-type functions for the Fe transition metal [26], so that it ensures a better performance than the conventional 6-31G(d) basis set for the iron atom of Fc, by providing a more appropriate description for the important energy differences between the atomic $3d^n4s^1$ and $3d^{n-1}4s^2$ configurations [27]. The present IR spectral simulations of the Fc conformers use the same model of B3LYP/m6-31G(d) *without any scaling*. The calculated *Fc IR spectra using the same method applied scaling factors of 0.9539 (eclipsed) and 0.9491 (staggered) for IR frequencies above 1200 cm^{-1} for the hydrocarbon vibration dominant motions.

The properties including the IR spectra, excess orbital energy spectrum (EOES) [28] and energy decomposition analysis (EDA) [29, 30] of *Fc and Fc conformers were also calculated in isolation. The former (EOES) uses the same B3LYP/m6-31G(d) model, but the latter (EDA) uses B3LYP/TZVP model. All calculations except for the EDA calculations are performed using the Gaussian16 computational chemistry package [31] and the EDA calculations are performed using Amsterdam Density Functional theory (ADF) [32].

3 Results and discussion

3.1 Geometry and conformer stability from methylation

It is well known that both *Fc and Fc (Fig. 1) exhibit eclipsed and staggered conformers with small energy differences [8, 10, 24]. The stability of staggered and eclipsed Fc conformers has been subjected to debate since the discovery some seventy years ago until very recently [6–8, 10, 12], when a series of combined experiment and theoretical research has provided compelling evidences that the eclipsed Fc in very low temperatures (under 18 K) is the more stable conformer [7, 10, 12]. Fc does not become a mixture of both eclipsed and staggered conformers [11], nor does it become an orientation with a mean rotation angle along the reaction coordinate. Instead, as the temperature is raised, higher vibrational states become populated along the reaction coordinate [7, 10] to populate additional vibrational models such as tilt. Most recently, Wang and Vasilyev provided further evidence for the temperature dependency of Fc conformers and their properties including IR spectra using molecular dynamics (MD) studies [12]. It was revealed that at higher temperatures such as room temperature of 25 °C (298.15 K), the cyclopentadienyl rings (Cp) of Fc exhibit apparent tilting up to 6° (at 293 K) [12].

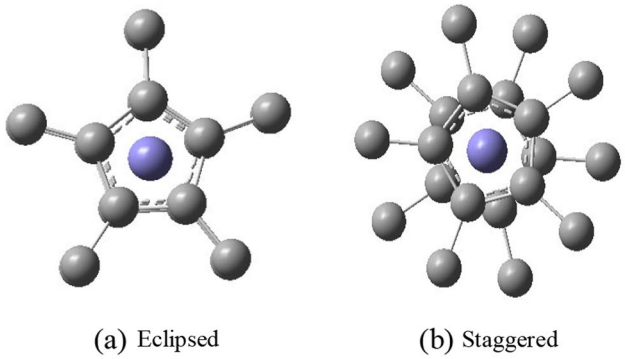

Fig. 1 Structures of eclipsed (**a**) and staggered (**b**) *Fc /Fc. In the case of *Fc, all carbons plus the centre Fe atom (no hydrogen) are presented dashed line the Cs bonded with Cp are methyl carbons, whereas in the case of Fc, all atoms, Hs and Cs and Fe are shown dashed line the atoms bonding with the pentagon Cp rings are hydrogens

Although the H's of cyclopentadienyl rings in Fc are replaced by methyl groups (–CH_3) in *Cp, the symmetry distortion is unlikely due to methyl torsion in *Cp at very low temperature (near 0 K) [8, 24]. As found in a recent inelastic neutron scattering (INS) spectroscopic study, Zachariou et al. [33] revealed that in gas phase, the methyl group of toluene undergoes almost free rotation, i.e., the rotational energy barrier is under 10 cm^{-1}, which is not the case in *Fc [19, 24]. Table 1 compares selected geometric and electronic properties of eclipsed and staggered Fc and *Fc. In a similar fashion, the eclipsed and staggered conformers of *Fc also exhibit a small energy difference as indicated

Table 1 Comparison of optimized geometric and electronic properties of *Fc conformers with Fc and literature

Parameter	*Fc [6]		Fc [6]		Exp (*Fc)		
	Eclipsed	Staggered	Eclipsed (D_{5h})	Staggered (D_{5d})	XAFS[a]	ED[b]	XC[c]
Fe–C_p (Å)	1.677	1.676	1.677	1.676	1.655	1.662	1.657
Fe–C (Å)	2.075	2.074	2.075	2.074	2.055	2.064	2.050
C–C, ring (Å)	1.435	1.435	1.435	1.435	1.431	1.439	1.419
C–C, (C–CH_3) (Å)	1.503	1.503	1.503	1.503	1.520	1.503	1.502
—H (Å)	1.096	1.096	1.096	1.096		1.115	
∡C_p–H (°)	4.690	4.030	4.690	4.030		3.450	
$<R^2>$ (a.u.)[d]	4994.88	4978.32	1358.84	1361.78			
α_{xx} (10^{-24} ESU)	368.8	368.6	175.4	176.2			
α_{yy} (10^{-24} ESU)	335.3	335.4	175.4	176.2			
α_{zz} (10^{-24} ESU)	335.3	335.3	203.7	203.7			
α_{xy} (10^{-24} ESU)	0.0	− 0.14	0.0	0.0			
α_{xz} (10^{-24} ESU)	0.0	− 0.12	0.0	0.0			
α_{yz} (10^{-24} ESU)	0.05	− 0.03	0.0	0.0			
α_0 (10^{-24} ESU)[e]	346.5	346.4	184.8	185.4			

[a]X-ray absorption fine structure (XAFS) [8, 9]

[b]Electron diffraction (ED) [23]

[c]X-ray crystallography (XC) [24]

[d]Total spatial extent $<R^2>$

[e]$\alpha_0 = (\alpha_{xx} + \alpha_{yy} + \alpha_{zz})/3$, approximate polarizability [36]

by experiments [8, 24]. However, several differences exist between the geometric parameters of the Fc conformer and the *Fc conformer. First, at *very low temperatures*, Fc is dominant by the eclipsed conformer with a point group symmetry of D_{5h} [6, 7, 10, 12]. Thermodynamics calculations with free energy correction at room temperature of 298.15 K do not change the energy order—the eclipsed Fc conformer exhibits a lower total energy, although vibrational levels along the reaction coordinate towards the staggered Fc conformer populate towards room temperature [10, 34]. Conversely, the staggered conformer of *Fc is more stable at low temperatures than the eclipsed counterparts [7, 8] but does not exhibit the exact D_{5d} and D_{5h} point group symmetry like unsubstituted Fc. The calculated energy difference in *Fc is very small (0.33 kcal mol^{-1}), in comparison with the ED measurement (1.03 kcal mol^{-1}) [35].

Table 1 compares the optimized geometric and electronic properties of *Fc conformers with Fc and with selected literature. There are no apparent differences in most geometric properties between the eclipsed and staggered Fc and *Fc in the calculations. For example, the Fe–Cp and Fe–C distances of the Fc and *Fc conformers are predicted to be 1.677 Å and 2.074 Å, respectively, in both cases. However, the C–C bond lengths in Cp ring of Fc conformers are most identical, whereas the same C–C bonds in the *Cp ring of *Fc exhibit small but apparent differences, leading to small differences in the ring perimeter [37] of *Cp ring for 7.178 Å and 7.177 Å, respectively, for eclipsed and staggered *Fc. The ring perimeters of *Fc are slightly expanded from the Fc conformers of 7.175 Å, in agreement with previous studies [8, 17, 20].

Our quantum mechanical calculations reveal that both Cp and *Cp are not perfect pentagons as their C–C bonds exhibit small discrepancies in the fourth significant figure. Small differences in C–C bond lengths in the CpH ring (C_{2v} point group symmetry) were hypothesised by low-temperature X-ray structural data [38] and suggested in our recent molecular dynamics (MD) study of Fc [12]. Experimental measurements are averaged over time under the conditions and the dynamics of Fc is temperature dependent. When methyl ($–CH_3$) substitutes the hydrogens in Fc, the *Fc conformers slightly distort from the high symmetry of Fc, leading to the C–CH_3 and C–H bond length and *Cp angles being distorted from D_5 point group. The symmetry of the pentamethylcyclopentadiene (*CpH) reduces to C_{2v} point symmetry (twofold rotational disorder). It is then possible that not all C–C bonds in the *Cp ring are equivalent. The C–C and C=C bonds exhibiting sp^3 and sp^2 hybridizations are claimed by a recent crystal structure determination (*CpH) [39]. In low-temperature phase (296 K), the crystal structure of *Fc was ordered with the staggered conformation, using single-crystal X-ray diffraction [24] which was confirmed by single-crystal neutron diffraction techniques (100 K) by Sanjuan-Szklarz et al. [40]. In the latter technique (neutron diffraction), the H-atom positions and their displacement parameters can be determined more accurately than from single-crystal X-ray radiation. Malischewski et al. [41] discovered that the Cp planes tilt in the eclipsed *Fc salts, in consonance with MD studies of Fc [12].

The bond lengths such as Fe–Cp (centroid), Fe–C, C–C and C–H and bond angles such as $\measuredangle C_p$–H of Fc and *Fc are virtually indistinguishable. However, some electronic properties such as the volumes and static polarizabilities of the *Fc conformers are significantly different from the Fc counterparts. For example, the electronic spatial extent ($<R^2>$) is a measure of spread of electron density over the molecule, which is directly proportional to the electronic volume of the molecule [42]. Table 1 exhibits the calculated electronic spatial extent $<R^2>$ of *Fc is nearly four times over that of Fc, 4993.38 a.u. versus 1358.84 a.u. (eclipsed). The volume expansion of *Fc due to the ten methyl groups is estimated approximately the volume of 3634.54 a.u. over ten methyls which is more than twice as large as ten times a single methyl group of approximately 1600 a.u. [43, 44]. Such significant volume differences between *Fc and Fc impact the nonlinear properties such as polarizability which is related to the volume [42].

The symmetry of the *Fc conformers distorts from the high symmetry of Fc. The Fc conformers take D_{5h} for eclipsed conformation and D_{5d} for staggered conformation in which the Cps are in an ideal pentagonal structure. The *Fc conformers distort from the exact D_{5h} and D_{5d} point group symmetry with approximately eclipsed and staggered structures, in agreement with experiments [8, 24]. The dipole moments of Fc conformers are zero, but a very small residual is presented for *Fc. The dipole moment is a simple global measure of the accuracy of electron density in a polar molecule, yet contains no information about the response of the ground state wave function to the electric field, since it can be computed from the zero-field density alone [36]. As a result, the infrared (IR) spectra of Fc can be very "clean" with only a few IR signals from induced dipole moments during vibration [6, 7, 10, 14]. The static polarizabilities, which are the first response of the electron density to electric fields, are also quite different between *Fc and Fc. It is not surprising that the total polarizability, α_0, of *Fc is significantly larger than Fc, as the *Fc with larger volumes ($<R^2>$) are more polarizable than smaller Fc. The nonzero off-diagonal polarizability residuals α_{ij} of the *Fc conformers in Table 1 indicate that the *Fc and Fc respond differently with respect to the application of an external field.

3.2 IR spectral response to methylation of the Cp rings

Far-IR spectra present the clearest signature of eclipsed and staggered conformations of Fc [6, 7, 10, 12]. The major

factors influencing the IR spectrum of a molecule include chemical bonds, atoms forming the bonds in the molecule and the three-dimensional (3D) structure of the compound. The greater the masses of the atoms involved in a bond, the lower the IR frequency at which the bond will absorb. As a result, it is expected that the replacement of the cyclopentadienyl rings (Cp) in Fc by the pentamethylcyclopentadienyl rings in *Cp will affect the IR spectrum of *Fc. The additional C–CH_3 bonds in *Fc which are not part of the *Cp rings contribute to the IR spectral signals of *Fc. Table 2 compares the calculated IR frequencies of the *Fc conformers with respect to IR frequency measurements in the solid state (in a pellet of a KBr disk) under low temperatures of 20 K [45] and 150 K [46].

There is a good agreement of the calculated IR frequencies (gas phase, 0 K) of *Fc with the IR spectrum of *Fc measured in crystal structure (150 K) [47, 48]. As pointed out by Arrais et al. [47], the measurement at 150 K does not show apparent differences from the IR spectrum measured in very low temperature of Duggan et al. [12]. Figure 2a, b compares the calculated IR spectra of Fc and *Fc in the eclipsed and staggered conformer forms, respectively, using the same DFT methods. Four apparent IR spectral bands (*A*, *B*, *C* and *D*) appear in *Fc at Band A with 400–500 cm^{-1}, Band B for < 1000 cm^{-1}, Band C for 1430–1550 cm^{-1} and Band D for 3000–3200 cm^{-1} regions. Relative intensities are presented in Fig. 2. The calculated IR bands of the *Fc conformers agree well with the measurements [12, 47, 48]. The comparison of calculated major IR transitions of *Fc conformers with the literature is provided in Table S3 in the Supplementary Material.

Excellent agreement of *Fc IR frequencies in Table 2 is achieved between the present study and previously calculated (staggered *Fc) [19] and measured [45, 46]. This is particularly the case in the low-frequency IR region of Bands *A* (**A*) and *B* (**B*) for $\nu < 1200$ cm^{-1}. The larger IR vibrational frequencies in the regions related to Bands *C* (**C*) and *D* (**D*) of $\nu > 1200$ cm^{-1}, are dominated by the organic moiety (*Cp) of *Fc where the scaling factors of 0.9539 and 0.9491 are applied for the eclipsed and staggered *Fc, respectively. As indicated by Gryaznova et al. [19], the vibrations above 1200 cm^{-1} are dominated by the methyl or methyl-Cp motion without significant centre metal Fe related motion. The basis set, m6-31G*, modifies the basis

Table 2 Comparison of major IR frequencies of *Fc conformers with measured FT-IR (cm^{-1})*

ν (cm^{-1})*	B3LYP/m6-31G(d)			Exp [45] (20 K)	Exp [46] (150 K)
	Eclipsed		Staggered		
	ν^a (cm^{-1}) scaling	ν (cm^{-1})*	ν^b (cm^{-1}) scaling		
200		202		200	200 (mw)
266		265		256	256 (mw)
386		389		375 (m)	381 (mw)
454		438		455 (s)	453 (s)
507		500		515 (mw)	515 (mw)
595		595		595 (w)	587 (mw)
1073		1073		1032 (ms)	1029 (m)
1106		1107		1075 (mw)	1070 (w)
1438	1362				1356 (w)
		1446	1372		1373 (s)
1465	1398	1466	1391	1378 (s)	1377 (s)
1526	1456	1485	1409	1428 (m)	1426 (m)
		1535	1456	1452 (m)	1449 (m)
		1538	1459		
1542	1471			1478 (m)	1473 (m)
					2713 (w)
					2854 (w)
3033	2893	3032	2878	2910 (vs)	2896 (s)
3096	2953	3095	2937	2960 (s)	2945 (w)
3124	2980	3123	2964	2980 (s)	2964 (m)

The experimental measurements were in solid state (KBr pellet disk). The full calculated IR spectra of the *Fc and Fc conformers are given in Table S2 of the Supplementary Material

*The DFT calculations (gas phase) include no scaling

[a]Applied a scaling factor of 0.9539 ($\upsilon > 1200$ cm^{-1})

[b]Applied a scaling factor of 0.9491 ($\upsilon > 1200$ cm^{-1})

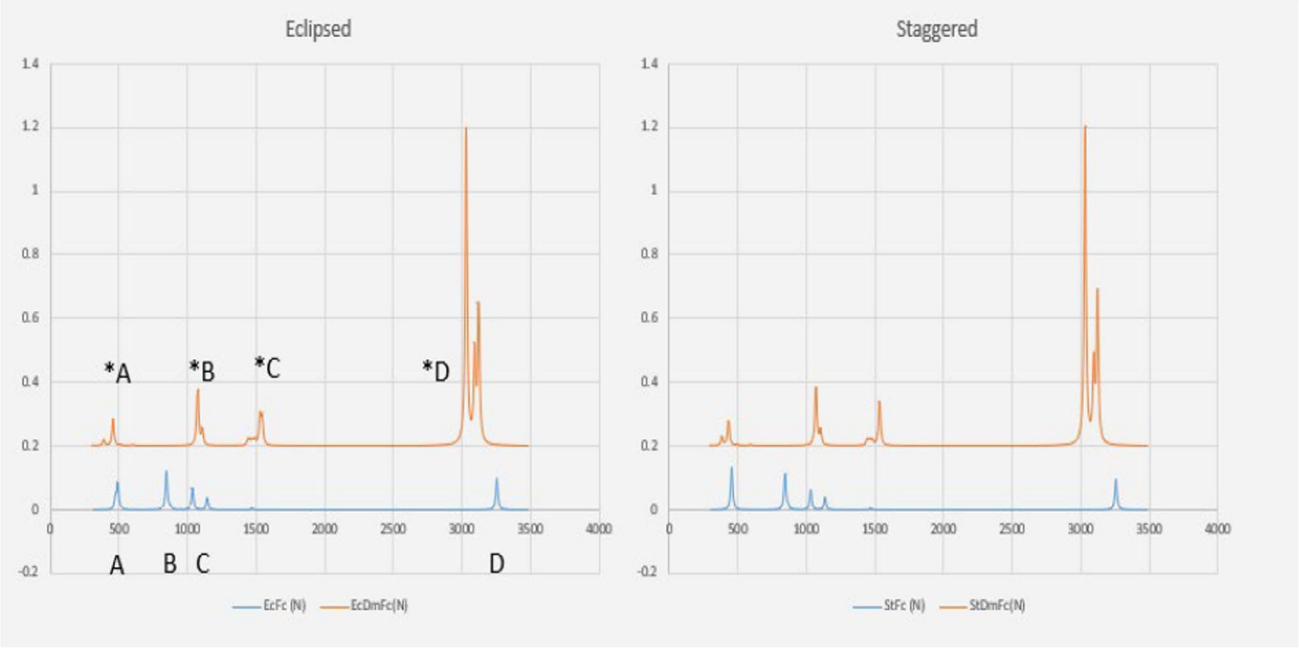

Fig. 2 Comparison of the calculated IR spectra of *Fc (orange) with respect to Fc (blue). **a** The eclipsed conformers. **b** The staggered conformers. Note in *Fc the staggered conformer is more stable but in Fc the eclipsed is more stable at low temperature

set of the centre metal Fe, so that in the IR region of above 1200 cm^{-1}, the m6-31G* basis set reduces to 6-31G* for H and C atoms and therefore, the calculated IR frequencies need scaling [19].

As we learned from IR spectral signatures of the Fc conformers [6, 7, 10], the small IR region (Bands A and B) is dominated by the vibrations related to the centre metal Fe where the modified m6-31G* basis set [26, 27] plays an important role. This modified 6-31G(d) basis set incorporates necessary diffuse d-type functions for Fe, exhibiting a better performance than the conventional 6-31G(d) basis set for the Fe atom in ferrocene by providing a more appropriate description for the important energy difference between the Fe atomic $3d^n4s^1$ and $3d^{n-1}4s^2$ configurations. The standard 6-31G(d) basis set is employed for other atoms such as carbons and hydrogens [27] in *Fc. The Bands *C and *D of $\nu > 1200$ cm^{-1} of *Fc, on the other hand, dominate by vibrations relating to the organic pentamethylcyclopentadienyl (*Cp) rings. The B3LYP/m6-31G(d) model for the *Cp moiety is ultimately the B3LYP/6-31G(d) model, and the scaling factors given in Table 2 are in vicinity of the same model for small organic molecules [48].

It is not surprising that the IR spectra of *Fc and Fc are different. However, the changes in IR spectra of the *Fc from Fc are not trivial—it is even more significant than the IR spectral differences between the eclipsed Fc and the staggered Fc [6]. Investigation of the IR spectra variation of *Fc with respect to Fc helps one to understand the property change related to the methylation of Fc. The calculated IR spectra of the *Fc conformers in Fig. 2 share some similarities with respect to the Fc conformers. The frequencies of the IR spectra in Fig. 2 are given in Table 2 without scaling. Both Fc and *Fc exhibit four major bands in their IR spectra, regardless of the conformers. The IR spectra of the eclipsed and staggered Fc are almost identical, except for the signature region of Band A 400–500 cm^{-1} [6, 7, 10]. Figure 2 shows that the IR spectral signature region of 400–500 cm^{-1} which is unique to Fc does not differentiate easily between the *Fc conformers because the IR spectral band splits in both eclipsed and staggered *Fc (Table 2). The IR spectra of the eclipsed and staggered *Fc exhibit only small differences in the entire IR region of 400–4000 cm^{-1} (see Figure S1 of the Supplementary Material). The largest shift is 16 cm^{-1} with accompanying change of oscillator strength for the band around 450 cm^{-1}; the next largest is a possible splitting around 1520–1540 cm^{-1} but with small changes in the oscillator strength. The IR spectra of Fc eclipsed and staggered conformers [6] are also provided in Figure S1 for reference. The calculated IR frequencies of *Fc conformers and the Fc conformers are provided in Table S3 in the Supplementary Material. Because the IR spectra of *Fc conformers are virtually indistinguishable at this time from the experimental evidence, the following discussion will focus on comparison of the staggered *Fc and Fc conformers (Fig. 2b).

In addition to the apparent differences between Fc and *Fc indicated above, several other differences between *Fc and Fc are observed from Fig. 2 and Table 2. First, the IR spectrum of *Fc is nearly seven times (Band *D) more intense than the IR spectrum of Fc. This is due to the small residual dipole moment in the *Fc caused by the symmetry distortion of the methyl groups, whereas the Fc are highly symmetric without permanent dipole moment. The IR absorption of Fc is due to the instantaneous transition dipole from asymmetric vibrations only, so that all vibration signals in the IR spectrum of Fc are relatively weak vibrations with similar intensities. By contrast, the most intense IR spectral band of *Fc is Band *D at $\nu \sim 3000$ cm^{-1} in the high-frequency region, due to the stretching vibrations of the methyl C–H bonds.

Second, the IR active spectral bands of *Fc and Fc exhibit different patterns which are unique to their structures. Only three of the four IR bands of *Fc and Fc are correlated—A and *A, C and *B, D and *D. The most intensive IR Band B in Fc (~ 850–880 cm^{-1}) is not active in *Fc, and the IR Band *C in *Fc is not active in Fc. This Band B in Fc consists of three nonzero vibrations with a signal at 848.07 cm^{-1} ($D = 286.22$ (10^{-40} esu^2 cm^2)) and a doubly degenerated signal at 871.11 cm^{-1} ($D = 8.80$ (10^{-40} esu^2 cm^2)) of the staggered Fc. The former is due to the vibrations that the Cp C–H bonds symmetrically wave up-down in the same direction, but the latter is due to the vibrations where the corresponding Cp C–H bonds wave asymmetrically up-down in opposite directions.

This Band B in Fc does not exist in *Fc, as there are no such C–H bonds where the carbons are part of the Cp ring in *Fc. One almost invisible "band" of Fc at approximately ~ 1440–1490 cm^{-1} of the in-plane C–H bond waving becomes significant in the IR spectrum of *Fc as Band *C, representing methyl (-CH_3) breathing vibrations. The band indicates that the role of pentamethylcyclopentadienyl rings (*Cp) in *Fc is not just a shift of the IR spectral bands of Fc but of significant structure-related changes. Band *C around 1530 cm^{-1} for the *Fc conformers, 1535 cm^{-1} (1527 cm^{-1} for eclipsed *Fc refer to Table 2) is dominated by the methyl in-plane bending/waving vibrations of the pentamethylcyclopentadieny rings of *Fc. The methyl groups do not exist in Fc conformers, as a result, this IR spectral band (*C) does not exist in the IR spectra of Fc conformers. Band C of Fc locates in the same region of Band *B of *Fc but splits into two well-separated peaks at ca 1035 cm^{-1} and 1141 cm^{-1}, respectively. The former (1035 cm^{-1}) for the Cp in-plane stretching turtle swimming [12]) and the latter (1141 cm^{-1}) for the opposite Cp ring breathing (small-large). The IR spectral band with largest frequency at around 3100–3200 cm^{-1}, refers to vibrations of the C–H stretches of the molecules. This band, Band *D of *Fc, refers to multiple methyl C–H stretch vibrations which are intense. In the same region, the Band D for the C–H stretch vibrations of Fc are degenerate due to the high symmetry.

The IR spectral differences between the eclipsed and staggered *Fc conformers are even less apparent than their Fc counterparts—the signature IR band between the eclipsed and staggered Fc [6, 7, 10], that is, the IR spectral splitting in the 400–500 cm^{-1} does not exist in the *Fc conformers anymore, as the IR spectra of both *Fc conformers splitting in this region. Interestingly, the calculated IR spectral splitting of the staggered *Fc of 62 cm^{-1} is larger than eclipsed *Fc of 53 cm^{-1}, in agreement with measured such splitting of 60–62 cm^{-1} [45–47]. This trend of IR spectral splitting is opposite to the Fc conformers where the eclipsed Fc IR band splitting apparently and such splitting of the staggered Fc is negligible. However, the IR spectral differences between the *Fc conformers need accurate experimental data with smart and novel design to serve as conformer signature. This IR spectral signature in Band A is unique to Fc.

3.3 Excess Fe-dominant orbital energies and EDA analysis

Other properties also experience changes to response methylation of the C–H bonds in Fc. One of such properties is measured using the excess orbital energy spectrum (EOES), which adequately reflects corresponding orbital energy variation between the eclipsed and staggered Fc ferrocene conformers [28]. It was found that the energies of the molecular orbitals (MOs) which are dominantly occupied by the 18 core electrons of Fe atom ($1s^2 2s^2 2p^6 3s^2 3p^6$) in Fc exhibit most significant changes in the inner electron shell between the Fc eclipsed and staggered conformers [28]. With respect to the conformational changes of Fc (where the Fe core electron dominant MOs of Fc), the Fe–$2p_z$ (3a) and Fe–$3p_z$ (16a) electrons along z-axis experience relatively small variations in their energies, comparing to other electrons in the same shell such as ($2s$) $2p_x$ and $2p_y$ and ($3s$) $3p_x$ and $3p_y$ [28] (Fig. 3).

Figure 4 reports the excess core/orbital electron energy spectrum (EOES) for the nine Fe core electron dominant MOs of *Fc with respect to Fc (i.e., $\Delta\varepsilon_i = \varepsilon_i$ (*Fc) - ε_i(Fc)). The EOES in Fig. 4 was applied to measure the methylation impact of *Fc from Fc (blue and orange bars) as well as the conformational changes of *Fc (green bars). Obviously, the methylation changes to the Fe core electrons are significant, it is over ten times with respect to the conformational changes of *Fc. The methylation changes (*Fc vs Fc) matter more in the z-axis (Cp–Fe–Cp axis) and the staggered conformer (orange bars in Fig. 4) changes slightly more than the eclipsed conformers (the blue bars in Fig. 4), particularly in the inner most core ($1s2s2p$) electrons. The $2p_z$ and $3p_z$ core electron energies of Fe change apparently larger than other Fe core electrons in the same shells in *Fc, which exhibits a

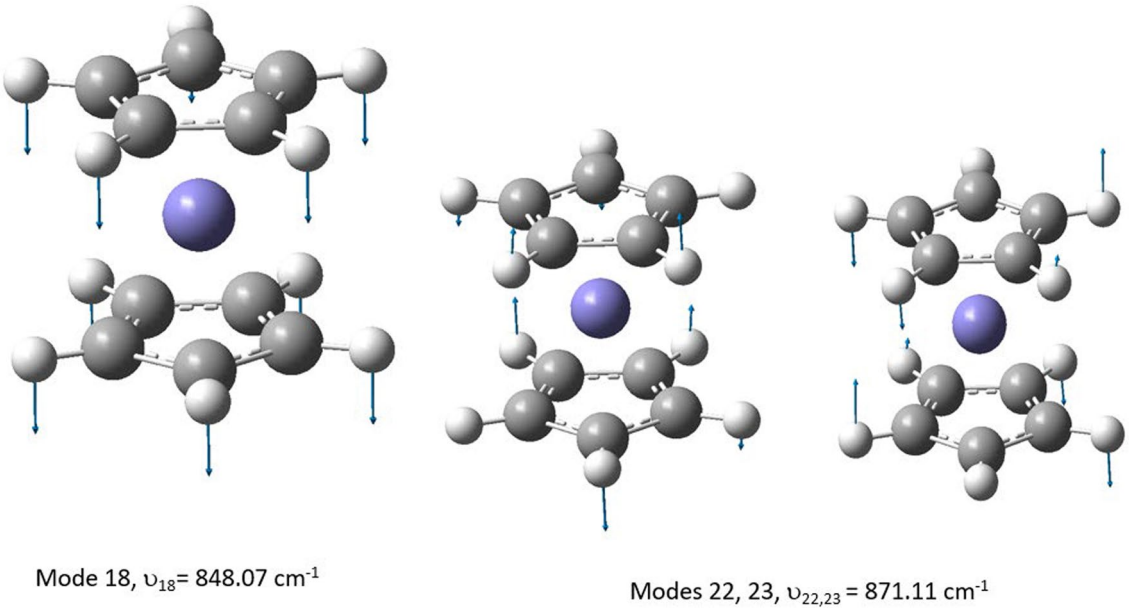

Fig. 3 Graphical presentation of the calculated vibrational modes of staggered ferrocene Band B (staggered)

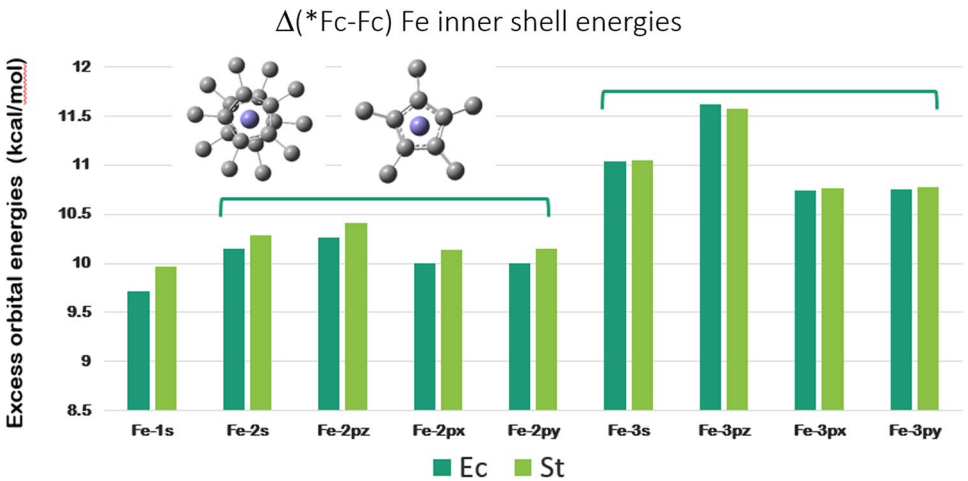

Fig. 4 Comparison of the Fe core electron response to methylation of Fc ($\Delta\varepsilon_i = \varepsilon_i^{*Fc} - \varepsilon_i^{Fc}$) in kcal/mol. The two units of (Fe–ns, Fe–np_z, Fe–np_x, Fe–np_y), where $n = 2$, 3 have the pattern

very different trend with respect to conformational changes which prefer the *xy*-plane.

Methylation of the C–H bonds in Fc impacts on the core electrons of Fe apparently. The methylation of Fc leads larger energy variation of outer Fe core electrons ($3s^2 3p^6$) than the inner core electrons ($1s^2 2s^2 2p^6$) for both conformers. For example, $\Delta\varepsilon_{3\delta} > \Delta\varepsilon_{2\delta} > \Delta\varepsilon_{1s}$ (here $\delta = s$, p_x, p_y and p_z) and the energy changes in Fe 1*s* orbital ($\Delta\varepsilon_{1s}$) is as large as 10 kcal mol^{-1} (i.e., $\Delta\varepsilon_{3s} > \Delta\varepsilon_{2s} > \Delta\varepsilon_{1s}$ and $\Delta\varepsilon_{3pz} > \Delta\varepsilon_{2pz}$) as shown in Fig. 4. Moreover, the staggered *Fc and Fc experience larger orbital energy variations than the eclipsed counterparts, which is particularly obvious in the inner most shell of Fe ($1s^2 2s^2 2p^6$). For example, the orange bars (staggered) are slightly larger than the blue bars (eclipsed) in the inner most region of Fe electrons ($1s^2 2s^2 2p^6$) in Fig. 4. Finally, the Fe electrons along the z-axis experience the largest energy changes in response to methylation of the C–H bonds, $\Delta\varepsilon_{npz} > \Delta\varepsilon_{npx}$, $\Delta\varepsilon_{npy}$, ($n = 2$ and 3). Therefore, although any such changes impact on all Fe core electrons of Fc and *Fc, methylation of Fc is along the *z*-axis whereas conformational changes (the green bars in Fig. 4) of *Fc happens in the *xy*-plane, i.e., $\Delta\varepsilon_{npz} < \Delta\varepsilon_{npx}$, $\Delta\varepsilon_{npy}$ ($n = 2$ and 3). The calculated inner shell reorganization energies (λ_{in}) of Fc and *Fc are given by 16 meV and 42 meV, respectively [49], also support the difference in the inner shells. The large Fe core electron energy change regarding methylation of Fc has been also revealed by the X-ray mass absorption coefficient of the materials (μ/ρ) in our previous fluorescence X-ray absorption fine structure (XAFS) measurements of Fc and *Fc [50]. Note that the absolute values [μ/ρ] for Fc

are larger than those of *Fc due to the larger percentage of Fe (~30%) in Fc than in *Fc (~17%).

As a result, unlike ferrocene ($C_{10}H_{10}Fe$), conformers of decamethylferrocene ($C_{20}H_{30}Fe$) do not possess exactly D_{5h} (eclipsed) and D_{5d} (staggered) point group symmetry. The *Fc is not a simple replacement of all hydrogens in Fc with ten methyl (-CH_3), but changes in *Fc include symmetry distortion such as unequal C–C bond lengths in the pentamethyl-cyclopentadienyls (*Cp), leading to small residual dipole moments, off-diagonal polarizabilities and more significantly, reversal of the conformer stability.

The interaction energy responses to the methylation of Fc are further explored using energy decomposition analysis (EDA). The EDA method, which is based on Morokuma [51] and the extended transition state (ETS) of Ziegler and Rauk [52], is the same as our previous study for EDA of Fc [30], which indicated that EDA energy components are dependent on the fragmentation schemes. In other words, EDA energy components are not uniquely defined quantities and are path functions [53]. Nevertheless, EDA is useful tool to compare the nature of bonds in closely related structures such as Fc. Table 3 reports the calculated energy components of the *Fc conformers together with the calculated energy components for the Fc conformers [30] for comparison. As pointed out in the EDA study of Fc [30] that the energy components obtained using the EDA depend on a number of factors including the fragmentation channels, the DFT functionals and the basis sets. In order to make a comparison, we employ the same method of Fc in the present study. That is, atomic fragment and B3LYP/TZ2P + methods [30].

Table 3 reveals that the energy components of the *Fc conformers with respect to previously obtained energies of the Fc conform using the same method, while the independent energy components of electrostatic energy, Pauli energy and orbital energy, that is, $\Delta(\Delta E_{estat})$, $\Delta(\Delta E_{Pauli})$ and $\Delta(\Delta E_{orb})$ of *Fc and Fc, exhibit the same attractive nature for the electrostatic and orbital energies, and repulsive nature of the Pauli energy. Contributions (percentages) to the total interaction energies with small differences, however, opposite signs, indicating that the more stable conformer of Fc and *Fc are not the same. For example, the total interaction energy $\Delta(\Delta E_{int})$ of the *Fc conformer pair is negative (− 0.4 kcal mol^{-1}), indicating staggered *Fc is the more stable conformer, whereas this energy the Fc conformer pair is positive (0.1 kcal mol^{-1}), suggesting that eclipsed Fc is the more stable conformer [30].

One of the most significant differences between the *Fc and Fc conformers is the nature of steric energies of the *Fc and Fc complexes which contribute to the reverse of the preferred conformer of the complexes at low temperature. In Fc, the steric energies of both eclipsed and staggered conformers are attractive (negative), indicating that the steric energy contribute to stabilize the Fc conformers [30]. This energy in *Fc, however, becomes very repulsive (positive), indicating that the methylated *Cp rings in *Fc leads to repulsive steric energy. As a result, the steric energy contributes to destabilise the *Fc complexes and makes the staggered *Fc the more stable conformer.

Steric energy is the sum of electrostatic energy (ΔE_{estat}) and quantum mechanical Pauli repulsive energy ($\Delta E_{Pauli.}$) of a compound. It is not a surprising that *Fc is responsible to larger steric repulsive energy due to the *Cp pairs. It is, however, still hardly to guess that how the large steric energy in *Fc changes in the electrostatic energy (ΔE_{estat}) and the quantum mechanical Pauli repulsive energy (ΔE_{Pauli}). The usually attractive ΔE_{estat} term corresponds to the classical electrostatic interaction between the unperturbed charge distributions of the prepared atoms. The Pauli repulsion ΔE_{Pauli} is the energy change associated with the transformation from the superposition of the unperturbed wave functions of the isolated atoms to the wave function, which properly obeys the Pauli principle through explicit antisymmetrization and renormalization of the product wave function [50]. It comprises the destabilizing interactions between electrons of the same spin on either atom. For example, while the electrostatic energy of *Fc is more attractive comparing to the same energy in Fc, as it is nearly doubled from that of Fc; the quantum mechanical Pauli energy of *Fc is approximately 70 times more repulsive in *Fc than in Fc.

Table 3 Comparison of energy terms for the eclipsed and staggered *Fc with respect to Fc.[a]

kcal mol^{-1}	*Fc			Fc		
	*Ec	*St	$\Delta^*(\Delta E_i)$	Ec	St	$\Delta(\Delta E_i)$
ΔE_{estat}	− 5310.1	− 5309.8	0.3	− 2793.1	− 2787.9	5.3
ΔE_{Pauli}	15,344.9	15,340.5	− 4.4	222.4	208.7	− 13.7
ΔE_{orb}	− 15,799.1	− 15,795.4	3.7	− 13,630.9	− 13,622.4	8.5
ΔE_{int} [b]	− 5764.3	− 5764.7	− 0.4	− 16,201.6	− 16,201.5	0.1
ΔE_{ster} [c]	10,034.8	10,030.7	− 4.1	− 2570.7	− 2579.12	− 8.4

[a]The BP86/TZ2P + model The same as the model used for Fc [30]

[b]$\Delta E_{int} = \Delta E_{estat} + \Delta E_{Pauli} + \Delta E_{orb}$

[c]$\Delta E_{ster} = \Delta E_{estat} + \Delta E_{Pauli}$

Figure 5 reports the decomposed energy contribution to the *Fc and Fc conformers. The attractive electrostatic energies of the *Fc conformers are not very different from the Fc conformers, whereas the contributions of the attractive orbital energies in *Fc conformer are apparently smaller the Fc counterparts. The most significant difference in energy contribution is the repulsive Pauli energies of *Fc which is some seventy times more than the Fc conformers. As a result, a large repulsive steric energy contribution destabilizes the methylated Fc. Hence, EDA might be a useful tool to compare the nature of bonds in closely related structures such as *Fc and Fc.

If the deviation of the alkyl groups from the ring plane is considered as a result of steric effects, it is probably due to steric interactions of methyl groups within each *Cp in *Fc. Increasing number of methyl substituents in the cyclopentadienyl rings of Fc results in the reverse of the eclipsed conformation to the staggered forms [49]. This conformational trend can be understood by their steric energy. The intra-Cp H···H (within a Cp) distances are ca. 2.70 Å for both eclipsed and staggered Fc, whereas the inter-Cp ring H···H' (between Cp and Cp') distances are 3.32 and 3.61 Å for eclipsed and staggered Fc, respectively. The latter, however, does not reverse the steric energy of the Fc conformers so that eclipsed conformer is the Fc preferred. In decamethylferrocene *Fc, the intra- and inter-ring repulsions are increased when methyl groups are introduced in the cyclopentadienyl rings. For a single *Cp(H)—ring, the crystal structure of an expected methyl orientation can be a "gear mesh" configuration in which one H of each methyl group is coplanar with the ring and equidistant from two of the hydrogens on an adjacent group [39, 54]. In *Fc, the adjacent methyl groups within one *Cp ring range are ca 2.28 Å (2.15 Å to 2.66 Å (average = 2.4 Å) in crystal) [54]. Between *Cp rings, the closest H···H' distances in *Fc range is ca 2.60 Å (2.49 Å to 3.41 Å (average = 2.6 Å) in crystal [54]). Thus, the H···H and H···H' distances *Fc conformers are apparently shorter than Fc conformers so that *Fc results in larger repulsive steric energy, reverses the stability of *Fc conformation.

Hydrogens on adjacent methyl groups of the same ring are ca. 0.3 Å closer than hydrogens on nearest-neighbour methyl groups on opposing rings in *Fc. As a result, the methyl groups in the *Cps of *Fc are not really "free rotations" but oriented to reduce the steric energy. It is found that the methyl orientations which minimize inter-ring methyl interactions (maximize the H···H' distances) will allow free rotation of methyl groups. However, the methyl orientations which minimize intra-ring methyl interactions (maximize the H···H distances) will allow free rotation of the *Cp rings [24]. The calculated H···H' and H···H for staggered *Fc are 2.594 Å and 2.284 Å, respectively, whereas for the eclipsed *Fc are 2.605 Å and 2.288 Å, respectively. Therefore, the methyl groups of *Fc do not subject to free rotation but take the same positions in both staggered and eclipsed *Fc in the present study as shown in Fig. 6 and the staggered *Fc with less steric repulsion is more stable conformer.

4 Conclusions

The present study reveals that methylation of Fc causes changes in the geometry, symmetry, IR spectrum and other electronic properties. These changes are rooted in the inner shell electrons dominated by the centre Fe atom, which is often beyond many measurables in *Fc and Fc. The present study reveals that the eclipsed and staggered conformers of *Fc experience symmetry distortion from strict high symmetry of exact D_{5h} (eclipsed) and D_{5d} (staggered) of Fc. Moreover, the C–C bond lengths of the pentacyclopentadienyl (*Cp) are not exactly the same, as supported by previous measurements [9, 41, 47, 55] and

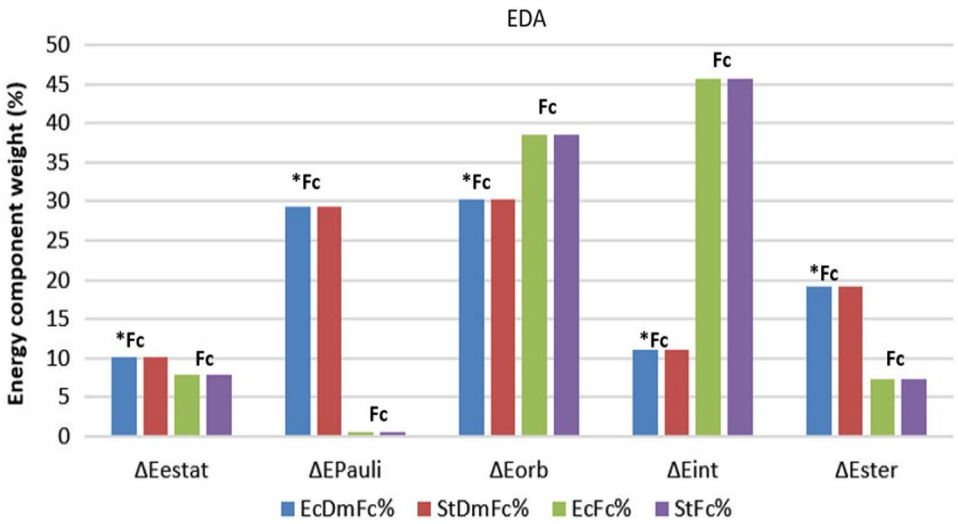

Fig. 5 Comparison of contributions of decomposed energies to the total energy in percentages of *Fc and Fc conformers. The data are based on Table 3

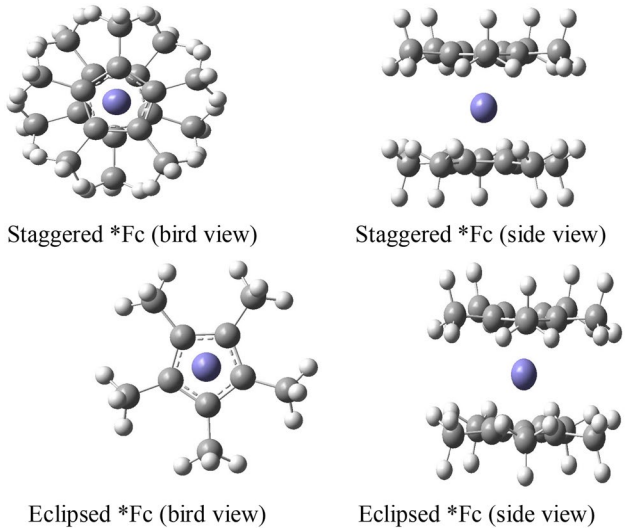

Fig. 6 Methyl orientations of the optimized structures of staggered (top) and eclipsed (bottom) decamethylferrocene (*Fc) in bird view and side view. Note the methyl position in the *Fc to minimize the steric energy

recent molecular dynamic simulation (MD) in higher temperatures of Fc [12]. Methylation of Fc leads to a stabilised staggered *Fc at low temperatures, in agreement with previous studies [8, 47].

Unlike for Fc, however, the IR spectrum does not provide a clear signature for *Fc, as it currently appears unable to differentiate staggered and eclipsed conformers of *Fc conclusively. Instead, the XAFS studies also using DFT have been shown to observe a difference in signature [9]. The IR spectra of *Fc and Fc are very different, the band at ~ 800 cm^{-1} of Fc due to the C–H vibrations of Cp disappears in *Fc, instead, a new IR band at ~ 1500 cm^{-1} due to C–CH_3 vibrations appears in *Fc. The most apparent enhancement of the IR spectral band in the ~ 3000 cm^{-1} region is due to the C–H methyl stretch vibrations in *Fc. Further analysis on the Fe core electrons ($1s^2 2s^2 2p^6$) using excess orbital energy spectrum (EOES) indicates that methylation of Fc causes approximately 10 eV energy changes with respect to their Fc counterparts. The large Fe core electronic structure changes in *Fc were seen in previous fluorescence X-ray absorption fine structure (XAFS) measurements of Fc and *Fc [9]. Moreover, the methylation impact on the Fe core electrons is directional—the Fe core electron energies of the Fe p_z orbitals along the *Cp–Fe–*Cp axis change more significantly than other Fe electrons in the same shell. Finally, the energy decomposition analysis (EDA) reveals that the significant increase (absolute value) of Pauli energy in *Fc contributes to the large repulsive steric energy in *Fc with respect to Fc counterparts. The present study provides a new direction of study ferrocene derivatives and other metallocenes.

Supplementary Information The online version contains supplementary material available at https://doi.org/10.1007/s00214-022-02949-8.

Acknowledgements FW would like to thank Dr V. Vasilyev and Dr S. Islam for their contributions to previous Fc studies which inspires this article. FW also thanks Swinburne University HPC facilities.

Author contributions FW wrote the main manuscript. All authors, both FW and CC reviewed the manuscript.

Funding Open Access funding enabled and organized by CAUL and its Member Institutions.

Data availability The data that support the findings of this study are available within the article and its supplementary materials.

Declarations

Competing interests The authors declare no competing interests.

Conflict of interest There are no conflicts of interest to declare.

References

1. Kealy TJ, Pauson PL (1951) A new type of organo-iron compound. Nature 168:1039
2. Wilkinson G et al (1952) The structure of iron bis-cyclopentadienyl. J Am Chem Soc 74:2125
3. Henize K, Lang H (2013) Ferrocene—beauty and function. Organometallics 32:5623
4. Seiwert B, Karst U (2008) Ferrocene-based derivatization in analytical chemistry. Anal Bioanal Chem 390:181
5. Singh A et al (2019) Ferrocene-appended pharmacophores: an exciting approach for modulating the biological potential of organic scaffolds. Dalton Trans 48:2840
6. Mohammadi N et al (2012) Differentiation of ferrocene D5d and D5h conformers using IR spectroscopy. J Organometal Chem 713:51–59
7. Best SP et al (2016) Reinterpretation of dynamic vibrational spectroscopy to determine the molecular structure and dynamics of ferrocene. Chem A Eur J 22:18019–18026
8. Bourke J et al (2016) Conformation analysis of ferrocene and decamethylferrocene via full-potential modeling of XANES and XAFS spectra. J Phys Chem Lett 7:2729–2796

9. Islam MT et al (2016) Accurate X-ray absorption spectra of dilute systems: absolute measurements and structural analysis of ferrocene and decamethylferrocene. J Phys Chem C 120:9399–9418
10. Trevorah RM et al (2020) Resolution of ferrocene and deuterated ferrocene conformations using dynamic vibrational spectroscopy: experiment and theory. Inorgan Chim Acta 506:119491
11. Kaspi-Kaneti AW, Tuvi-Arad I (2018) Twisted and bent out of shape: symmetry and chirality analysis of substituted ferrocenes. Organometallics 37:3314
12. Wang F, Vasilyev V (2020) Molecular dynamics study of ferrocene topology under various temperatures. Int J Quant Chem 120:e26398
13. Bear JC, Cockcroft JK, Williams JH (2020) Influence of solvent in crystal engineering: a significant change to the order-disorder transition in ferrocene. J Am Chem Soc 142:1731
14. Lippincott ER, Nelson RD (1958) The vibrational spectra and structure of ferrocene and ruthenocene. Spectrochim Acta 10:307
15. Sanderson CT et al (2002) Classical metallocenes as photoinitiators for the anionic polymerization of an alkyl 2-cyanoacrylate. Macromolecules 35:9648
16. Cotton FA, Wilkinson G (1988) Advanced inorganic chemistry, 5th edn. Wiley, New York
17. Coriani S et al (2006) The equilibrium structure of ferrocene. ChemPhysChem 7:245
18. Roy DR, Duley S, Chattaraj PK (2008) Bonding, reactivity and aromaticity in some novel all-metal metallocenes. Proc Indian Natl Sci Acad 74:11
19. Gryaznova TP et al (2010) DFT study of substitution effect on the geometry, IR spectra, spin state and energetic stability of the ferrocenes and their pentaphospholyl analogues. J Organometal Chem 695:2586
20. Bean DE, Fowler PW, Morris MJ (2011) Aromaticity and ring currents in ferrocene and two isomeric sandwich complexes. J Organometal Chem 696:2093
21. King RB, Bisnette MB (1967) Organometallic chemistry of the transition metals XXI. Some π-pentamethylcyclopentadienyl derivatives of various transition metals. J Organometal Chem 8:287
22. Struchkov YT et al (1978) Crystal and molecular structures of two polymethylferrocenes: octamethylferrocene and decamethylferrocene. J Organometal Chem 145:213
23. Almenningen A et al (1979) The molecular structure of decamethylferrocene studied by gas phase electron diffraction. Determination of equilibrium conformation and barrier to internal rotation of the ligand rings. J Organometal Chem 173:293
24. Freyberg DP et al (1979) Crystal and molecular structures of decamethylmanganocene and decamethylferrocene. Static Jahn-Teller distortion in a metallocene. J Am Chem Soc 101:892
25. Gerasimova TP, Katsyuba SA (2015) Infrared and Raman bands of cyclopentadienyl ligands as indicators of electronic configuration of metal centers in metallocenes. J Organometal Chem 776:30
26. Mitin AV, Baker J, Pulay P (2003) An improved 6–31G* basis set for first-row transition metals. J Chem Phys 30:7775–7782
27. Martin J, Baker J, Pulay P (2009) Comments on the molecular geometry of ferrocene: the dangers of using quantum chemistry programs as black boxes. J Comput Chem 30:881–883
28. Islam S, Wang F (2015) The d-electrons of Fe in ferrocene: the excess orbital energy spectrum (EOES). RSC Adv 5:11933–11941
29. Wolters LP, Bickelhaupt FM (2005) The activation strain model and molecular orbital theory. Wiley Interdiscip Rev Comput Mol Sci 5:324
30. Wang F, Islam S, Vasilyev V (2015) Ferrocene orientation determined intramolecular interactions using energy decomposition analysis. Materials 8:7723
31. Frisch MJ, Trucks GW, Schlegel HB, Scuseria GE, Robb MA, Cheeseman JR, Scalmani G, Barone V, Petersson GA, Nakatsuji H, Li X, Caricato M, Marenich AV, Bloino J, Janesko BG, Gomperts R, Mennucci B, Hratchian HP, J. V. (2016) Gaussian 16, Revision C.01. Gaussian Inc, Wallingford CT
32. Gusarov S, van den Hoek FEHP, Jacob CR, Jacobsen H, Jensen L, Kaminski JW, van Kessel G, Kootstra F, Kovalenko A, Krykunov MV et al (2020) ADF2020. Vrije Universiteit, Amsterdam
33. Zachariou A, Hawkins AP, Collier P et al (2020) The methyl torsion in unsaturated compounds. ACS Omega 5:2755
34. Xu Z-F, Xie Y, Feng W-L, Schaefer HF (2003) Systematic investigation of electronic and molecular structures for the first transition metal series metallocenes M(C5H5)2 (M = V, Cr, Mn, Fe Co, and Ni). J Phys Chem A 107:2716
35. Haaland A, Nilsson JE (1968) The determination of barriers to internal rotation by means of electron diffraction. Ferrocene and ruthenocene. Acta Chem Scand 22:2653
36. Haita D, Head-Gordon M (2018) How accurate are static polarizability predictions from density functional theory? An assessment over 132 species at equilibrium geometry. Phys Chem Chem Phys 20:19800
37. Wickrama Arachchilage AP, Wang Y, Wang F (2011) A quantum mechanical study of bioactive 3-chloro-2,5-dihydroxybenzyl alcohol through substitutions. Theor Chem Acc 130:965
38. Haumann T, Benet-Buchholz J, Boese R (1996) Structural effects of spiroconjugation: crystal structures of spiro[4.4]nonatetraene and spiro[4.4]nona-1,3,7-triene. J Mol Struct 374:299
39. Benda C, Klein W, Fässler TF (2017) Crystal structure of 1,2,3,4,5-pentamethyl-1,3-cyclopentadiene, C10H16. Zeitschrift für Kristallographie New Cryst Struct 232:511
40. Sanjuan-Szklarz WF et al (2016) Yes, one can obtain better quality structures from routine X-ray data collection. Int Union Crystallogr J 3:61
41. Malischewski M et al (2016) Isolation and structural and electronic characterization of salts of the decamethylferrocene dication. Science 353:678–682
42. Maity R, Mandal B, Misra A (2019) Effect of donor acceptor substitution position on the electrical responsive properties of Azulene system: a computational study. Mol Phys 14:1781
43. Falzon CT, Wang F (2005) Understanding glycine conformation through molecular orbitals. J Chem Phys 123:214307
44. Falzon CT, Wang F, Pang WN (2006) Orbital signatures of methyl in L-alanine. J Phys Chem B 110:9713
45. Duggan DM, Hendrickson DN (1975) Electronic structure of various ferricenium systems as inferred from Raman, infrared, low-temperature electronic absorption, and electron paramagnetic resonance measurements. Inorgan Chem 14:955–970
46. Stanghellini PL et al (2000) The charge distribution on metal-bonded cyclopentadienyl rings from infrared intensities. J Organometal Chem 593:36–43
47. Arrais A et al (2003) Solid-state adducts between C60 and decamethylferrocene. Eur J Inorgan Chem 6:1186–1192
48. Kesharwani MK, Brauer B, Martin JML (2015) Frequency and zero-point vibrational energy scale factors for double-hybrid density functionals (and other selected methods): can anharmonic force fields be avoided? J Phys Chem A 119:1701
49. Gryaznova TP, Katsyuba SA, Milyukov VA, Sinyashin OG (2010) DFT study of substitution effect on the geometry, IR spectra, spin state and energetic stability of the ferrocenes and their pentaphospholyl analogues. J Organometal Chem 695:2586
50. Andrada DM, Foroutan-Nejad C (2020) Phys Chem Chem Phys 22:22459
51. Morokuma K (1971) Molecular orbital studies of hydrogen bonds. III. C=O...H–O hydrogen bond in $H_2CO...H_2O$ and $H_2CO...2H_2O$. J Chem Phys 55:1236–1244
52. Ziegler T, Rauk A (1977) On the calculation of bonding energies by the Hartree Fock Slater method. Theor Chem Acc 46:1–10

53. Andrada DM, Foroutan-Nejad C (2020) Energy components in energy decomposition analysis (EDA) are path functions; why does it matter? Phys Chem Chem Phys 22:22459
54. Freyberg DP, Robbins JL, Raymond KN, Smart JC (1979) Crystal and molecular structures of decamethylmanganocene and decamethylferrocene. Static Jahn-Teller distortion in a metallocene. J Am Chem Soc 101:892
55. Gomez-Sandoval Z, Peña E, Guerra CF, Bickelhaupt FM, Mendez-Rojas MA, Merino G (2009) A helicoid ferrocene. Inorgan Chem 48:2714–2716